Inorg. Chem. **2005**, *44*, 5921–5933

Intra- and Intermolecular N–H···F–C Hydrogen-Bonding Interactions in Amine Adducts of Tris(pentafluorophenyl)borane and -alane

Andrew J. Mountford,[†] Simon J. Lancaster,*[,†] Simon J. Coles,[‡] Peter N. Horton,[‡] David L. Hughes,[†] Michael B. Hursthouse,[‡] and Mark E. Light[‡]

Wolfson Materials and Catalysis Centre, School of Chemical Sciences and Pharmacy, University of East Anglia, Norwich, NR4 7TJ U.K., and School of Chemistry, University of Southampton, Highfield, Southampton, SO17 1BJ U.K.

Received April 29, 2005

The reaction between $B(C_6F_5)_3$ and NH_3(g) in light petroleum yielded the solvated adduct $H_3N{\cdot}B(C_6F_5)_3{\cdot}NH_3$. Treatment with a second equivalent of $B(C_6F_5)_3$ afforded $H_3N{\cdot}B(C_6F_5)_3$. Attempts to prepare the analogous alane adduct were unsuccessful and resulted in protolysis. Related compounds of the form $R'R''N(H){\cdot}M(C_6F_5)_3$ were synthesized from $M(C_6F_5)_3$ and the corresponding primary and secondary amines (M = B, Al; R′ = H, Me, CH_2Ph; R″ = Me, CH_2Ph, CH(Me)(Ph); R′R″ = *cyclo*-C_5H_{10}). The solid-state structures of 13 new compounds have been elucidated by single-crystal X-ray diffraction and are discussed. Each of the borane adducts has a significant bifurcated intramolecular hydrogen bond between an amino hydrogen and two *o*-fluorines, while N–H···F–C interactions in the alane adducts are weaker and more variable. ^{19}F NMR studies demonstrate that the borane adducts retain the bifurcated C–F···H···F–C hydrogen bond in solution. Compounds of the type $R'R''N(H){\cdot}M(C_6F_5)_3$ conform to Etter's rules for the prediction of hydrogen-bonding interactions.

Introduction

The inorganic fluoride ion is one of the best hydrogen-bond acceptors, with the hydrogen bond in the bifluoride anion (HF_2^-) approaching the strength of a covalent bond.[1] In contrast, the C−F group is a poor hydrogen-bond acceptor, and until the late 1990s, there were relatively few reported examples of interactions in which organofluorine might be regarded as accepting of a hydrogen bond.[2] The controversy surrounding close X−H···F−C contacts has been the subject of a number of detailed analyses.[3−5] Dunitz concluded that organofluorine rarely accepts hydrogen bonds and suggested that in order to be regarded as a hydrogen bond the H···F distance should be significantly shorter than the sum of the van der Waals radii (ca. 2.55 Å) and preferably no longer than ca. 2.2−2.3 Å, with obtuse H−F−C angles.

Intermolecular X−H···F−C interactions are believed to play a role in certain biological recognition processes and have been investigated as synthons in organic crystal engineering.[6,7] Interest in X−H···F−C interactions has coincided with intense academic research into pentafluorophenyl compounds of the group 13 elements, particularly tris(pentafluorophenyl)borane, because of their importance in catalysis both as activators for single-site transition-metal polymerization catalysts[8] and as Lewis acid catalysts for organic transformations.[9] Inevitably, studies of this nature

* To whom correspondence should be addressed. E-mail: S.Lancaster@uea.ac.uk. Tel: +44 1603 592009. Fax: +44 1603 592003.
† University of East Anglia.
‡ University of Southampton.

(1) Harrell, S. A.; McDaniel, D. H. *J. Am. Chem. Soc.* **1964**, *86*, 4497.
(2) Shimoni, L.; Glusker, J. P. *Struct. Chem.* **1994**, *5*, 383.
(3) (a) Howard, J. A. K.; Hoy, V. J.; O'Hagan, D.; Smith, G. T. *Tetrahedron* **1996**, *52*, 12613. (b) Plenio, H.; Diodone, R. *Chem. Ber.* **1997**, *130*, 633. (c) Takemura, H.; Kon, N.; Yasutake, M.; Nakashima, S.; Shinmyozu, T.; Inazu, T. *Chem. Eur. J.* **2000**, *6*, 2334. (d) Brammer, L.; Bruton, E. A.; Sherwood, P. *Cryst. Growth Des.* **2001**, *1*, 277. (e) Hyla-Kryspin, I.; Haufe, G.; Grimme, S. *Chem. Eur. J.* **2004**, *10*, 3411.
(4) Dunitz, J. D.; Taylor, R. *Chem. Eur. J.* **1997**, *3*, 89.
(5) An alternative description of the attractive interaction between N−H and F−C dipoles has recently been proposed: (a) Snyder, J. P.; Chandrakumar, N. S.; Sato, H.; Lankin, D. C. *J. Am. Chem. Soc.* **2000**, *122*, 544. (b) Lankin, D. C.; Grunewald, G. L.; Romero, F. A.; Oren, I. Y.; Snyder, J. P. *Org. Lett.* **2002**, *4*, 3557.
(6) (a) O'Hagan, D.; Rzepa, H. S. *Chem. Commun.* **1997**, 645. (b) Hoffmann, M.; Rychlewski, J. *J. Am. Chem. Soc.* **2001**, *123*, 2308.
(7) (a) Borwick, S. J.; Howard, J. A. K.; Lehmann, C. W.; O'Hagan, D. *Acta Crystallogr. E* **1997**, *53*, 124. (b) Weiss, H.-C.; Boese, R.; Smith, H. L.; Haley, M. M. *Chem. Commun.* **1997**, 2403. (c) Thalladi, V. K.; Weiss, H.-C.; Bläser, D.; Boese, R.; Nangia, A.; Desiraju, G. R. *J. Am. Chem. Soc.* **1998**, *120*, 8702. (d) Barbarich, T. J.; Rithner, C. D.; Miller, S. M.; Anderson, O. P.; Strauss, S. H. *J. Am. Chem. Soc.* **1999**, *121*, 4280. For a recent review of fluorine in crystal engineering, see: (e) Reichenbächer, K.; Süss, H. I.; Hulliger, J. *Chem. Soc. Rev.* **2005**, *34*, 22.

10.1021/ic050663n CCC: $30.25
Published on Web 07/14/2005

Chart 1[a]

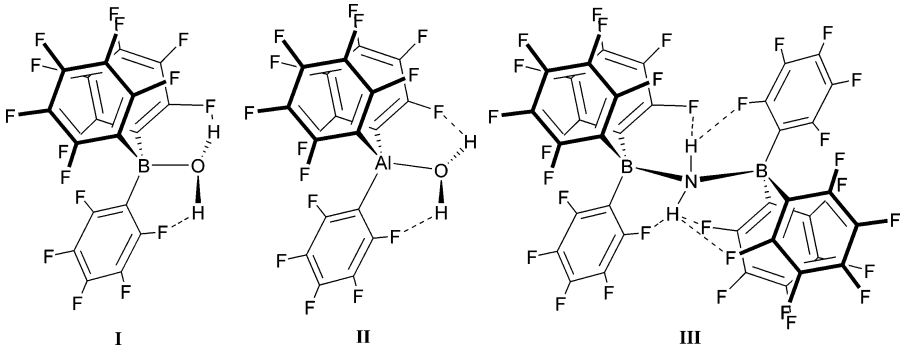

I II III

[a] Intermolecular O−H···F−C interactions in **I** and **II** have been omitted.

have led to the characterization of a great number of Lewis base adducts.[10] Protic Lewis bases experience an increase in Brønsted acidity and hydrogen-bond donor strength upon adduct formation. Perhaps the most obvious and best studied example is $H_2O{\cdot}B(C_6F_5)_3$ (**I**, Chart 1),[11] which has an estimated pK_a of 8.4 in acetonitrile.[10c] The aluminum analogue $H_2O{\cdot}Al(C_6F_5)_3$ (**II**) has recently been reported and is one of the relatively few examples of Lewis base adducts of $Al(C_6F_5)_3$.[12]

We recently described the synthesis and structure of the amidodiborate anion $[H_2N\{B(C_6F_5)_3\}_2]^-$ (**III**), in which there is a complex intramolecular hydrogen-bonding arrangement.[13] Further studies directed toward extending this family of anions have involved the isolation of examples of primary and secondary amine adducts of $B(C_6F_5)_3$ in which a NH group participates in a bifurcated hydrogen-bonding arrangement.[14−16] The hydrogen-bonding patterns observed in these preliminary studies of boron complexes prompted further investigation of their structural chemistry. We became interested in whether similar patterns would be observed with amine adducts of $Al(C_6F_5)_3$. Herein we report the synthesis and solid-state structures of a number of novel protic amine adducts of $B(C_6F_5)_3$ and $Al(C_6F_5)_3$ and contrast the intramolecular hydrogen-bonding patterns.

Scheme 1[a]

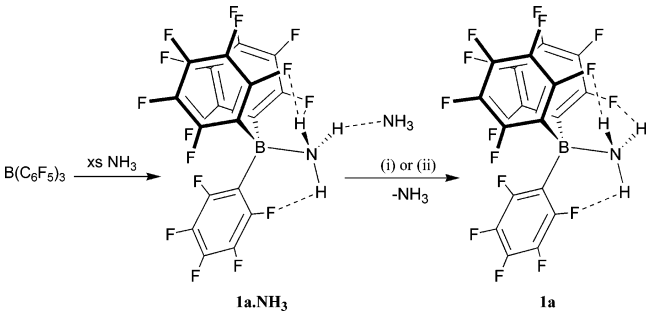

[a] (i) $B(C_6F_5)_3$. (ii) Dissolution in toluene and removal of volatiles under vacuum.

Results

The ammonia adduct $H_3N{\cdot}B(C_6F_5)_3$ was among the first complexes of $B(C_6F_5)_3$ reported, but to date, the solid-state structure has not been described.[17] Using a procedure similar to that employed by Stone, NH_3(g) was bubbled through a light petroleum solution of $B(C_6F_5)_3$, precipitating a colorless solid (Scheme 1). Characterization by multinuclear NMR (benzene-d_6) confirmed that this crude material was indeed an adduct, in which the ^{11}B NMR resonance was high-field-shifted from δ 59 for free $B(C_6F_5)_3$ to δ −7. However, the ^{1}H NMR spectrum consisted of two broad resonances of approximately equal intensity at δ 3.71 and δ −0.57. The N−H stretching region of the FT-IR spectrum was complex, and bands were observed at 3396, 3373, 3362, 3330, and 3296 cm^{-1}. Recrystallization from a dichloromethane/light petroleum mixture yielded colorless crystals that retained the spectroscopic characteristics of the crude material. Elemental analysis gave a C−N ratio of close to 18:2, suggesting a composition with two nitrogens to each boron atom. We therefore formulated the product as $H_3N{\cdot}B(C_6F_5)_3{\cdot}NH_3$ (**1a**·NH_3), in which a second ammonia molecule is hydrogen-bonded to the adduct. The solid-state structure (which is

(8) Chen, E. Y.-X.; Marks, T. J. *Chem. Rev.* **2000**, *100*, 1391. Bochmann, M.; Lancaster, S. J.; Hannant, M. D.; Rodriguez, A.; Schormann, M.; Walker, D. A.; Woodman, T. J. *Pure Appl. Chem.* **2003**, *75*, 1183. Bochmann, M. *J. Organomet. Chem.* **2004**, *689*, 3982.

(9) Ishihara, K.; Yamamoto, H. *Eur. J. Org. Chem.* **1999**, 527.

(10) For example, see: (a) Lesley, M. J. G.; Woodward, A.; Taylor, N. J.; Marder, T. B.; Cazenobe, I.; Ledoux, I.; Zyss, J.; Thornton, A.; Bruce, D. W.; Kakkar, A. K. *Chem. Mater.* **1998**, *10*, 1355. (b) Jacobsen, H.; Berke, H.; Döring, S.; Kehr, G.; Erker, G.; Fröhlich, R.; Meyer, O. *Organometallics* **1999**, *18*, 1724. (c) Bergquist, C.; Bridgewater, B. M.; Harlan, C. J.; Norton, J. R.; Friesner, R. A.; Parkin, G. *J. Am. Chem. Soc.* **2000**, *122*, 10581. (d) Beckett, M. A.; Brassington, D. S.; Light, M. E.; Hursthouse, M. B. *J. Chem. Soc., Dalton Trans.* **2001**, 1768. (e) Drewitt, M. J.; Niedermann, M.; Kumar, R.; Baird, M. C. *Inorg. Chim. Acta* **2002**, *335*, 43. (f) Vagedes, D.; Erker, G.; Kehr, G.; Bergander, K.; Kataeva, O.; Fröhlich, R.; Grimme, S.; Mück-Lichtenfeld, C. *Dalton Trans.* **2003**, 1337.

(11) Doerrer, L. H.; Green, M. L. H. *J. Chem. Soc., Dalton Trans.* **1999**, 4325.

(12) Chakraborty, D.; Chen, E. Y.-X. *Organometallics* **2003**, *22*, 207.

(13) Lancaster, S. J.; Rodriguez, A.; Lara-Sanchez, A.; Hannant, M. D.; Walker, D. A.; Hughes, D. L.; Bochmann, M. *Organometallics* **2002**, *21*, 451.

(14) Lancaster, S. J.; Mountford, A. J.; Hughes, D. L.; Schormann, M.; Bochmann, M. *J. Organomet. Chem.* **2003**, *680*, 193.

(15) Mountford, A. J.; Hughes, D. L.; Lancaster, S. J. *Chem. Commun.* **2003**, 2148.

(16) Resconi and co-workers recently reported the reaction of protic aromatic N-heterocycles with $B(C_6F_5)_3$. For comparison, they also prepared (2,3-dihydro-1*H*-indole)tris(pentafluorophenyl)boron, which exhibits a bifurcated intramolecular hydrogen-bonding motif closely related to those in this study: Guidotti, S.; Camurati, I.; Focante, F.; Angellini, L.; Moscardi, G.; Resconi, L.; Leardini, R.; Nanni, D.; Mercandelli, P.; Sironi, A.; Beringhelli, T.; Maggioni, D. *J. Org. Chem.* **2003**, *68*, 5445.

(17) Massey, A. G.; Park, A. J.; Stone, F. G. A. *Proc. Chem. Soc.* **1963**, 212. Massey, A. G.; Park, A. J. *J. Organomet. Chem.* **1964**, *2*, 245.

presented below) was elucidated by X-ray crystallography and confirmed the proposed composition. Retention of the second NH_3 molecule during recrystallization, despite the very low solubility of NH_3 in dichloromethane at room temperature, indicates that the hydrogen-bonding interaction is maintained in solution. Similar behavior has been reported for the hydrate, $H_2O{\cdot}B(C_6F_5)_3$ (**I**), which forms intermolecular associations and cocrystallizes with solvent molecules that provide hydrogen-bond acceptors.[18] **I** has also been shown to interact further with water molecules in a toluene solution.[19]

Treatment of **1a**·NH_3 with a second equivalent of $B(C_6F_5)_3$ (Scheme 1) leads to the formation of a new adduct with only one ^{1}H NMR resonance at room temperature and a C−N ratio of 18:1, indicating the composition $H_3N{\cdot}B(C_6F_5)_3$ (**1a**). We find that **1a** is more conveniently isolated by preparing **1a**·NH_3 in toluene, removing the volatiles under reduced pressure, and recrystallizing the resulting solid from dichloromethane/light petroleum. Compound **1a** was also characterized by X-ray crystallography, and the significant structural features are discussed below.

The reported chemistry of $Al(C_6F_5)_3$ differs from $B(C_6F_5)_3$ in that it forms adducts with arenes, is poorly soluble in hydrocarbons, and decomposes in chlorocarbons,[20−22] while there are relatively few reports of Lewis base adducts.[12,23−25] Our attempts to prepare an aluminum analogue of **1a** were ultimately unsuccessful. Treatment of a colorless light petroleum suspension of $Al(C_6F_5)_3$ with NH_3(g) resulted in the slow formation of a sticky yellow solid, which proved to be insoluble in dichloromethane. When the reaction with NH_3(g) was performed in benzene-d_6 and monitored by ^{1}H NMR, the formation of the yellow precipitate was found to be accompanied by generation of C_6F_5H. In light of the successful isolation of $H_3N{\cdot}B(C_6F_5)_3$, $H_2O{\cdot}Al(C_6F_5)_3$,[12] and the primary and secondary adducts **2b**−**g** described below, the evident instability of $H_3N{\cdot}Al(C_6F_5)_3$ toward protolysis is somewhat surprising.

Treatment of $B(C_6F_5)_3$ with the primary amines H_2N^tBu (**b**), H_2NCH_2Ph (**c**), and $H_2NCH(Me)Ph$ (**d**) and secondary amines $HNMe_2$ (**e**), *cyclo*-$(H)NC_5H_{10}$ (**f**), $HNMeCH_2Ph$ (**g**), and $HN(PhCH_2)_2$ (**h**) in a dichloromethane or toluene solution results in the formation of adducts **1b**−**h** (Scheme 2). The syntheses and solid-state structures of **1e** and **1f** have been described elsewhere, and we have previously reported the synthesis and spectroscopic characterization of **1b**.[13,14,26] The new adducts **1c**, **1d**, **1g**, and **1h** have been characterized by ^{1}H, ^{13}C, ^{11}B, and ^{19}F NMR spectroscopy, elemental analyses, and single-crystal X-ray diffraction. The ^{11}B NMR resonances at δ −4.2 (**1c**), −4.4 (**1d**), −1.2 (**1g**), and −0.3 (**1h**) [cf. δ −5.2 (**1b**), −1.4 (**1e**), and −2.1 (**1f**)] are characteristic of four-coordinate neutral adducts of $B(C_6F_5)_3$.

Scheme 2

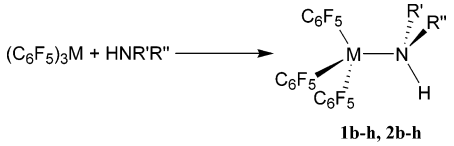

1b-h, 2b-h

1, M = B; **2**, M = Al;
b, R' = H, R" = ^{t}Bu; **c**, R' = H, R" = CH_2Ph;
d, R' = H, R" = CH(Me)Ph;
e, R' = R" = Me; **f**, R'R" = *cyclo*-C_5H_{10};
g, R' = Me, R" = CH_2Ph; **h**, R' = R" = CH_2Ph

Table 1. δ(N−H) for the Amines HNR′R″ and Adducts HR′R″N·M$(C_6F_5)_3$ (Benzene-d_6, 20 °C)

	δ(N*H*R′R″)/ppm		
amine	free amine	borane adduct (**1**)	alane adduct (**2**)
a, NH_3		2.67	
b, H_2N^tBu	0.77	4.29	3.92
c, H_2NCH_2Ph	0.86	4.42	3.26
d, $H_2NC(Me)(H)Ph$	0.99	5.25, 4.02	3.29
e, $HNMe_2$	0.23	6.23	2.76
f, *cyclo*-$(H)NC_5H_{10}$	0.87	5.13	2.68
g, $HNMeCH_2Ph$	0.71	5.91	4.30
h, $HN(CH_2Ph)_2$	1.09	6.36	3.99

The aluminum analogues **2b**−**h** were prepared in toluene solutions at room temperature (Scheme 2). The crude products were subsequently recrystallized from dichloromethane/light petroleum mixtures at −25 °C to yield, for all but **2g**, crystallographic quality colorless crystals. Because $Al(C_6F_5)_3$ decomposes in a dichloromethane solution, the stability of the reaction product toward recrystallization from dichloromethane is itself evidence for the formation of stable adducts.[22] ^{1}H, ^{13}C, and ^{19}F NMR and elemental analyses of **2b**−**h** were also consistent with adduct formation. We note that while $H_2O{\cdot}Al(C_6F_5)_3$ and $H(Me)O{\cdot}Al(C_6F_5)_3$ have half-lives of 33 and 193 h, respectively, in a toluene solution, no evolution of C_6F_5H was observed during the characterization of **2b**−**h**, indicating that at 20 °C the adducts are indefinitely stable with respect to intra- or intermolecular protolysis reactions.

For both the borane and alane adducts, the ^{1}H NMR resonance of the NH group exhibits a dramatic change in chemical shift upon adduct formation. Table 1 presents the δ(N*H*) resonance for the free amine, the borane adducts, and the alane adducts. The greatest values of $\Delta\delta(NH_{adduct} - NH_{free\ amine})$ are found for the secondary amine borane

(18) For compounds of the form $[H_2O{\cdot}B(C_6F_5)_3]{\cdot}L_x$, see the following. (a) For $L_x = 2H_2O$: Danopoulos, A. A.; Galsworthy, J. R.; Green, M. L. H.; Cafferkey, S.; Doerrer, L. H.; Hursthouse, M. B. *Chem. Commun.* **1998**, 2529. (b) For $L_x = {}^t$BuOH: Reference 10c. (c) For $L_x = Me_2SO_2{\cdot}H_2O$: Coles, S. J.; Hursthouse, M. B.; Beckett, M. A.; Dutton, M. *Acta Crystallogr. E* **2003**, *59*, 1354. (d) For $L_x = Et_2O$, H_2O: Lancaster, S. J.; O'Hara, S. M.; Bochmann, M. In *Metalorganic Catalysts for Synthesis and Polymerization*; Kaminsky, W., Ed.; Springer Verlag: Berlin, 2000.

(19) Beringhelli, T.; Maggioni, D.; D'Alfonso, G. *Organometallics* **2001**, *20*, 4927.

(20) Free $(C_6F_5)_3Al$ presents a significant explosion hazard if subjected to thermal or physical shock and was therefore isolated only on a small scale by the reaction of $(C_6F_5)_3B$ with Me_3Al in a light petroleum solution followed by removal of the volatiles and resuspension in light petroleum. See: Reference 21.

(21) Biagini, P.; Lugli, G.; Abis, L.; Andreussi, P. U.S. Patent 5,602,269, 1997. Lee, C. H.; Lee, S. J.; Park, J. W.; Kim, K. H.; Lee, B. Y.; Oh, J. S. *J. Mol. Catal., A* **1998**, *132*, 231.

(22) Chakraborty, D.; Chen, E. Y.-X. *Inorg. Chem. Commun.* **2002**, *5*, 698.

(23) Belgardt, T.; Storre, J.; Roesky, H. W.; Noltemeyer, M.; Schmidt, H.-G. *Inorg. Chem.* **1995**, *34*, 3821.

(24) Bolig, A. D.; Chen, E. Y.-X. *J. Am. Chem. Soc.* **2001**, *123*, 7943.

(25) LaPointe, R. E.; Roof, G. R.; Abboud, K. A.; Klosin, J. *J. Am. Chem. Soc.* **2000**, *122*, 9560.

(26) Schatte, G.; Chivers, T.; Tuononen, H. M.; Suontamo, R.; Laitinen, R.; Valkonen, J. *Inorg. Chem.* **2005**, *44*, 443.

Table 2. ν(N−H) for Selected Amines HNR′R″ and Adducts HR′R″N·M(C_6F_5)$_3$

amine	ν(N−H)/cm^{-1} free amine	borane adduct (**1**)[a]	alane adduct (**2**)[a]
a, NH_3	3434, 3334[c]	3373, 3362, 3296	
b, H_2N^tBu	3350, 3277[b]	3346	3299, 3254
c, H_2NCH_2Ph	3367, 3294[b]	3337, 3282	3315, 3273
e, $HNMe_2$	3347[c]	3330	3302
f, *cyclo*-(H)NC_5H_{10}	3272[b]	3312	3274
g, $HNMeCH_2Ph$	3322[b]	3318	3278
h, $HN(CH_2Ph)_2$	3307[b]	3315	3259

[a] Nujol mull. [b] At high dilution in CCl_4. [c] Gas phase.

adducts, in which we know the NH is engaged in a bifurcated hydrogen-bonding interaction (see below). $\Delta\delta$ is somewhat less for the primary amine borane adducts, in which only one of the two NH's is strongly hydrogen-bonded. The alane adducts give lower values of $\Delta\delta$, which is presumably due, at least in part, to weaker intramolecular hydrogen bonding.

Selected compounds have been characterized by IR spectroscopy, and the ν(N−H) values are collated in Table 2. The secondary amine adducts give a single sharp N−H stretch, while with the exception of **1b**, the primary amine adducts exhibit distinguishable symmetric and asymmetric stretches. In general, the stretching frequencies are some 30−50 cm^{-1} lower for the aluminum compounds when compared to their boron analogues. However, aside from the borane versus alane shift, there is no distinctive trend on coordination. The data for the free amine, run at high dilution to eliminate intermolecular hydrogen bonding, are given in Table 2. Hydrogen bonding would be expected to lead to lower values of ν(N−H) than those found for the isolated amine molecule, but we do not observe a distinctive correlation between ν(N−H) and the extent of intramolecular hydrogen bonding (as elucidated by the X-ray studies described below) and an explanation for this awaits further investigation.

Crystallography

The hitherto unreported solid-state structures of the borane adducts **1a**−**d**, **1a**·NH_3, **1g**, and **1h** and the new aluminum compounds **2b**−**g** have been determined by crystallographic methods. Views of the boron compounds, **1a**·NH_3, **1a**−**d**, **1g**, and **1h**, are shown in Figures 1−7, and those of the aluminum compounds, **2b** and **2d**−**g**, in Figures 8−13 (see also the Supporting Information). The structures of the borane adducts are similar in as far as the geometries about all of the boron and nitrogen atoms are essentially tetrahedral. We note a characteristically small C−B−C angle, ca. 105°, between the two C_6F_5 groups linked in a bifurcated hydrogen-bond scheme (see below); the other C−B−C angles are ca. 114°. There is little variation in bond lengths, and these are summarized in Table 3. The overall mean bond lengths are 1.646(2) Å for B−C and 1.635(4) Å for B−N and lie within the range previously reported for related adducts.[14−16] There are also only minor variations from tetrahedral geometry in the alane adducts; for the rings involved in bifurcated hydrogen-bonding systems, the C−Al−C angles are now in

Table 3. Selected Bond Lengths; Mean (or Unique) Values, in Å, with Standard Deviations (or Estimated Standard Deviations) in Parentheses

compd no.	no. of independent molecules	distance mean B−C	mean B−N	mean N−C
1a·NH_3	1	1.637(1)	1.606(3)[a]	
1a	2	1.636(2)	1.624(1)	
1b	2	1.646(5)	1.645(1)	1.550(1)
1c	1	1.642(3)	1.625(2)[a]	1.505(2)[a]
1d	1	1.651(3)	1.638(6)[a]	1.535(6)[a]
1e	2	1.654(2)	1.653(1)	1.506(1)
1f	2	1.658(5)	1.630(1)	1.515(3)
1g	1	1.648(7)	1.635(8)[a]	1.506(6)
1h	1	1.645(6)	1.651(2)[a]	1.514(6)

compd no.	no. of independent molecules	distance mean Al−C	mean Al−N	mean N−C
2b	1	2.005(4)	1.997(2)[a]	1.531(2)[a]
2c	2	1.9952(13)	1.976(2)	1.5105(5)
2d	1	1.993(2)	1.987(2)[a]	1.508(4)[a]
2e	4	1.998(2)	1.971(4)	1.494(3)
2f	2	1.997(2)	1.975(3)	1.504(2)
2g	2	1.991(2)	1.967(2)	1.506(3)

[a] A unique value, with its estimated standard deviation in parentheses; all other values are mean values, with standard deviations.

the range 106−111° but are still significantly less than the other C−Al−C angles. The mean Al−C distance 1.997(2) Å is similar to those of the basic adducts of Al(C_6F_5)$_3$ reported to date: THF·Al(C_6F_5)$_3$,[23] MMA·Al(C_6F_5)$_3$,[24] H_2O·Al(C_6F_5)$_3$, and H(Me)O·Al(C_6F_5)$_3$.[12] At 1.979(5) Å, the mean Al−N bond length is slightly longer than that in the anion [(C_6F_5)$_3$Al(imidazole)Al(C_6F_5)$_3$]$^-$, which is 1.911(2) Å.[25]

In all of the borane and alane adducts, with the exception of **2d**, the arrangement of bonds about the B−N or Al−N bond is staggered, and there are few examples where the trans torsion angle differs by more than 10° from 180°. The exception **2d** (Figure 9) shows an eclipsed arrangement, with a C−Al−N−C torsion angle of −1.3(2)°, and we suggest that this results from a combination of the favorable overlap of the phenyl ring C(3−8) with one of the C_6F_5 rings C(21−26) and the overlap of the other C_6F_5 rings with symmetry-related rings in neighboring molecules.

Where there are corresponding structures of the boron and aluminum compounds, we find that although the Al/B−(C_6F_5)$_3$ units are very similar, there may be variation in the arrangements of the amine groups, as is seen in the NH_2-CHMePh groups of **1d** and **2d**. In the compounds with symmetrical amine groups, for example, the $NHMe_2$ groups of **1e** and **2e** and the *cyclo*-(H)NC_5H_{10} groups in **1f** and **2f**, the pseudo mirror symmetry in these ligands extends into the B/Al−(C_6F_5)$_3$ groups; in all of these compounds, there is one C_6 ring with a N−B/Al−C−C torsion angle of almost 90° and two others twisted about 30° in opposite directions. There is disorder in one of the C_6F_5 groups in one molecule of **2f**, but the general scheme of pseudosymmetry is maintained. In **1b/2b**, **1c/2c**, and **1g/2g**, there are significant differences between the conformations of the boron and aluminum analogues, presumably resulting from the increased N−Al vs N−B bond distances, the flexibility of the

Table 4. Short Hydrogen Atom Contacts and Hydrogen Bond Dimensions, in Å and Degrees[a]

D−H···A	*d*(D−H)	*d*(H···A)	*d*(D···A)	∠(DHA)	symmetry operation	
			Compound **1a**·NH_3			
N(1)−H(1n)···F(5)	0.87(3)	2.40(3)	2.982(3)	124(3)		
N(1)−H(2n)···N(2)	0.93(4)	1.96(4)	2.876(3)	172(3)	*	
N(1)−H(2n)···F(15)	0.93(4)	2.57(3)	2.655(3)	85(2)		
N(1)−H(2n)···F(15^{I})	0.93(4)	2.73(3)	2.998(3)	98(2)	*	I: $1-x, 2-y, -z$
N(1)−H(3n)···F(2^{II})	0.87(4)	2.59(4)	3.280(3)	137(3)	*	II: $x-{}^{1}/_{2}, 1{}^{1}/_{2}-y, z-{}^{1}/_{2}$
N(1)−H(3n)···F(10)	0.87(4)	2.16(4)	2.767(3)	127(3)		
N(1)−H(3n)···F(15)	0.87(4)	2.22(4)	2.655(3)	110(3)		
N(1)−H(3n)···F(15^{I})	0.87(4)	2.49(4)	2.998(3)	117(3)	*	I: $1-x, 2-y, -z$
N(2)−H(5n)···F(7^{III})	0.87(5)	2.64(4)	3.114(4)	115(4)	*	III: $x-{}^{1}/_{2}, 1{}^{1}/_{2}-y, {}^{1}/_{2}+z$
N(2)−H(5n)···F(10^{I})	0.87(5)	2.51(5)	3.375(4)	172(4)	*	I: $1-x, 2-y, -z$
N(2)−H(6n)···F(4^{IV})	0.82(5)	2.47(5)	3.170(3)	144(3)	*	IV: $1-x, 1-y, -z$
			Compound **1a**			
N(1)−H(1a)···F(2)	0.91	2.44	2.630(2)	91.6		
N(1)−H(1a)···F(8)	0.91	2.18	2.747(2)	119.8		
N(1)−H(1b)···F(14)	0.91	2.27	2.870(2)	122.9		
N(1)−H(1b)···F(29)	0.91	2.52	2.981(2)	111.6	*	
N(1)−H(1b)···F(36^{I})	0.91	2.34	3.117(2)	142.9	*	I: $x, y-1, z$
N(1)−H(1c)···F(2)	0.91	2.28	2.630(2)	102.6		
N(1)−H(1c)···F(28)	0.91	2.39	3.270(2)	163.0	*	
N(21)−H(21a)···F(9^{I})	0.91	2.38	2.954(2)	121.2	*	II: $x-1, 1+y, z$
N(21)−H(21a)···F(17^{II})	0.91	2.43	3.011(2)	122.1	*	III: $x-1, y, z$
N(21)−H(21a)···F(32)	0.91	2.24	2.865(2)	125.3		
N(21)−H(21b)···F(22)	0.91	2.39	2.636(2)	95.1		
N(21)−H(21b)···F(23^{IV})	0.91	2.38	3.201(2)	150.8	*	IV: $-x, 1-y, 1-z$
N(21)−H(21b)···F(38)	0.91	2.13	2.742(2)	123.8		
N(21)−H(21c)···F(18^{V})	0.91	2.31	3.160(2)	154.3	*	V: $x-1, y, z$
N(21)−H(21c)···F(22)	0.91	2.32	2.636(2)	99.8		
			Compound **1b**			
N(1)−H(1a)···F(2)	0.92	2.15	2.770(2)	123.4		
N(1)−H(1a)···F(8)	0.92	2.15	2.808(2)	127.3		
N(1)−H(1b)···F(14)	0.92	2.44	3.017(2)	121.0		
N(1)−H(1b)···F(44^{I})	0.92	2.55	3.232(2)	131.2	*	I: $x, 1+y, z$
N(31)−H(31a)···F(48)	0.92	2.58	3.128(2)	118.3		
N(31)−H(31b)···F(36)	0.92	2.20	2.832(2)	124.9		
N(31)−H(31b)···F(42)	0.92	2.11	2.756(2)	126.5		
			Compound **1c**			
N(1)−H(1na)···F(9^{I})	0.89(2)	2.26(2)	3.0282(11)	145(2)	*	I: ${}^{1}/_{2}-x, {}^{1}/_{2}+y, {}^{1}/_{2}-z$
N(1)−H(1nb)···F(6)	0.86(2)	2.12(2)	2.723(2)	127(2)		
N(1)−H(1nb)···F(11)	0.86(2)	2.23(2)	2.747(2)	118.3(15)		
			Compound **1d**			
N(4)−H(4a)···F(16)	0.90	2.40	2.988(5)	123		
N(4)−H(4a)···F(35^{I})	0.90	2.44	3.226(5)	144	*	I: $1{}^{1}/_{2}-x, y-{}^{1}/_{2}, {}^{1}/_{2}-z$
N(4)−H(4b)···F(26)	0.90	2.32	2.770(5)	111		
N(4)−H(4b)···F(32)	0.90	2.16	2.819(5)	129		
			Compound **1e**			
N(4)−H(4)···F(22)	0.91	2.15	2.755(3)	123		
N(4)−H(4)···F(32)	0.91	2.10	2.751(4)	128		
N(8)−H(8)···F(62)	0.91	2.10	2.737(4)	126		
N(8)−H(8)···F(72)	0.91	2.09	2.731(3)	126		
			Compound **1f**			
N(4)−H(4)···F(12)	0.91	2.10	2.747(2)	127		
N(4)−H(4)···F(26)	0.91	2.10	2.733(2)	126		
N(8)−H(8)···F(52)	0.91	2.11	2.758(2)	128		
N(8)−H(8)···F(66)	0.91	2.14	2.745(2)	123		
			Compound **1g**			
N(1)−H(1n)···F(5)	0.92(5)	2.10(5)	2.725(6)	125(3)		
N(1)−H(1n)···F(11)	0.92(5)	2.15(5)	2.763(6)	123(4)		
			Compound **1h**			
N(1)−H(1)···F(6)	0.93	2.22	2.790(2)	118.9		
N(1)−H(1)···F(11)	0.93	2.02	2.710(2)	129.5		
			Compound **2b**			
N(4)−H(4a)···F(12)	0.90	2.28	2.953(2)	132		
N(4)−H(4b)···F(36)	0.90	2.14	2.891(2)	140		
			Compound **2c**			
N(1)−H(1n)···F(5)	0.92(3)	2.47(3)	2.943(2)	112(2)		
N(1)−H(1n)···F(5^{I})	0.92(3)	2.43(3)	3.337(2)	167(2)	*	I: $1-x, -y, 1-z$
N(1)−H(1n)···F(15)	0.92(3)	2.36(3)	2.879(2)	116(2)		
N(2)−H(3n)···F(21)	0.90(2)	2.48(2)	2.835(2)	104(2)		
N(2)−H(3n)···F(30)	0.90(2)	2.43(2)	2.897(2)	112(2)		
N(2)−H(3n)···F(30^{II})	0.90(2)	2.40(2)	3.298(2)	173(2)	*	II: $2-x, 1-y, 1-z$
N(2)−H(4n)···F(20)	0.98(3)	2.49(3)	3.006(2)	113(2)		

Table 4 (Continued)

D−H···A	*d*(D−H)	*d*(H···A)	*d*(D···A)	∠(DHA)	symmetry operation	
			Compound **2d**			
N(1)−H(1d)···F(18^{I})	0.92	2.43	3.086(3)	128.5	*	I: $-x, -y, 2-z$
N(1)−H(1d)···F(20)	0.92	2.47	2.970(3)	114.5		
N(1)−H(1e)···F(14)	0.92	2.37	3.126(3)	139.4		
N(1)−H(1e)···F(16^{II})	0.92	2.55	3.304(3)	139.8	*	II: $1+x, y, z$
			Compound **2e**			
N(1)−H(1)···F(1)	0.93	2.49	3.001(4)	115.2		
N(1)−H(1)···F(6)	0.93	2.36	2.916(4)	118.2		
N(1)−H(1)···F(26^{I})	0.93	2.34	3.114(4)	140.0	*	I: $1+x, y, 1+z$
N(2)−H(2)···F(14^{II})	0.93	2.55	3.283(4)	136.5	*	II: $x, y, z-1$
N(2)−H(2)···F(16)	0.93	2.20	2.929(4)	134.3		
N(3)−H(3)···F(31)	0.93	2.26	2.906(4)	126.2		
N(3)−H(3)···F(45)	0.93	2.47	3.013(4)	117.6		
N(3)−H(3)···F(52^{III})	0.93	2.38	3.107(4)	134.6	*	III: $1-x, {}^{1}/_{2}+y, 1-z$
N(4)−H(4)···F(41^{IV})	0.93	2.51	3.266(4)	139.0	*	IV: $-x, y-{}^{1}/_{2}, 1-z$
N(4)−H(4)···F(46)	0.93	2.38	2.925(4)	117.1		
			Compound **2f**			
N(41)−H(41)···F(16)	0.91	2.39	2.944(2)	120		
N(41)−H(41)···F(26)	0.91	2.29	2.912(2)	125		
N(81)−H(81)···F(62)	0.91	2.34	2.926(2)	122		
N(81)−H(81)···F(72)	0.91	2.39	2.933(2)	119		
			Compound **2g**			
N(1)−H(1)···F(6)	0.93	2.34	2.906(2)	119.0		
N(31)−H(31)···F(32)	0.93	2.51	3.021(3)	114.7		
N(31)−H(31)···F(48)	0.93	2.49	2.989(3)	113.6		

[a] An asterisk indicates an intermolecular interaction. Estimated standard deviations are in parentheses.

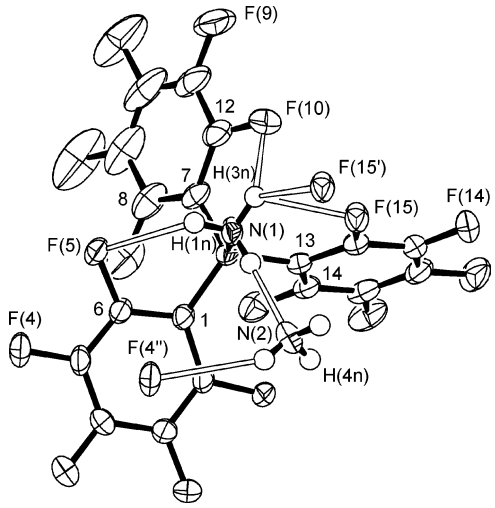

Figure 1. Molecular structure of **1a**·NH_3 with displacement ellipsoids at the 50% probability level.

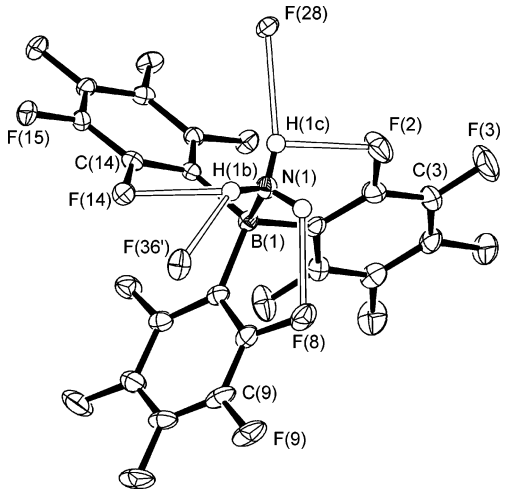

Figure 2. Molecular structure of one of the two independent but very similar molecules of **1a** with displacement ellipsoids at the 50% probability level.

three C_6F_5 rings, the bulk of the amine group, the competition from intermolecular interactions, and not least the relative tendency toward the formation of intramolecular N−H···F interactions.

To some extent all of the complexes reported here exhibit N−H···F interactions. The intra- and intermolecular contacts are listed in Table 4. We define short H···F contacts as those less than 2.2 Å, medium length between 2.2 and 2.35 Å, and longer contacts where the distance is between 2.35 and 2.55 Å (the last being the sum of van der Waals' distances). The short H···F interactions in particular fulfill the Dunitz criteria for classification as hydrogen bonds.[4]

The presence of a short [1.96(4) Å] nearly linear [172-(3)°] H···N hydrogen bond is responsible for the stability of **1a**·NH_3 (Figure 1). This second sphere adduct is reminiscent of a number of reported $[H_2O{\cdot}B(C_6F_5)_3]{\cdot}L_x$ structures.[18] Second-coordination-sphere association through hydrogen bonding between ammonia molecules is somewhat less common than that for water but has been previously described for complexes of the alkaline-earth metals.[27] Of the remaining hydrogens, the second engages in a bifurcated F···H···F interaction and the third has only a long (2.45 Å) contact. Significantly, this pattern is similar to that of the primary amine adducts (**1b**−**d**) described below.

The H atoms of the NH_3 groups in the unsolvated adduct **1a** (Figure 2) are involved in a complex series of intra- and intermolecular H···F interactions.[28] Each of the hydrogens has a short- or medium-length intramolecular contact to a single *o*-F. H(1b) and H(1c) form further medium-length interactions with fluorines from neighboring molecules. The

(27) Rossmeier, T.; Reil, M.; Korber, N. *Inorg. Chem.* **2004**, *43*, 2206.

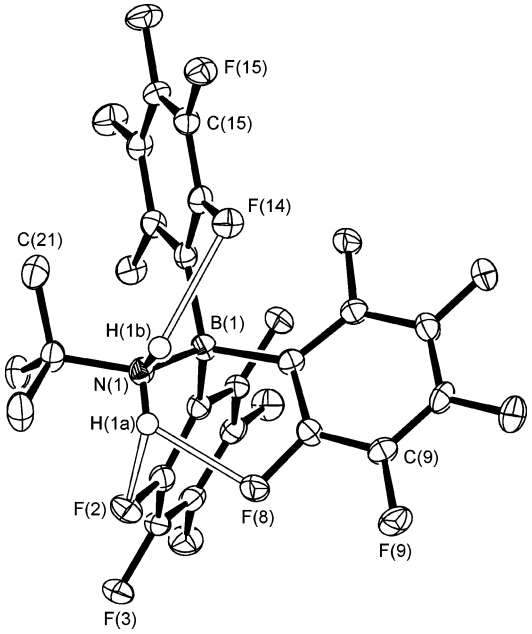

Figure 3. Structure of one of the two molecules of **1b** with displacement ellipsoids at the 50% probability level. C-bonded H atoms are omitted for clarity.

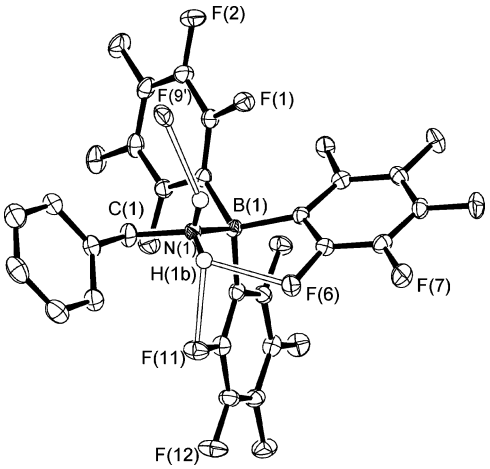

Figure 4. Molecular structure of **1c** with displacement ellipsoids at the 50% probability level. C-bonded H atoms are omitted for clarity.

solid-state structure of **1a** therefore has a number of features in common with the monohydrate $H_2O{\cdot}B(C_6F_5)_3$ (**I**, Chart 1),[11] in which each of the H atoms forms one short intramolecular and one longer intermolecular hydrogen bond to fluorine atoms.

The molecular structures of the three primary amine adducts of $B(C_6F_5)_3$, **1b**−**d** (Figures 3−5), exhibit very similar principal intramolecular hydrogen-bonding interactions. In each case, one H is engaged in a bifurcated interaction with two short−medium contacts to *o*-F's.[29] The average H···F contact distance for the bifurcated hydrogen

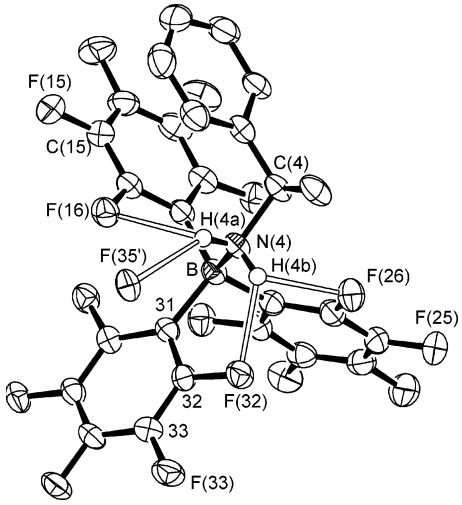

Figure 5. Molecular structure of **1d** with displacement ellipsoids at the 50% probability level. C-bonded H atoms are omitted for clarity.

increases in line with the steric bulk of the alkyl group **1b** < **1c** < **1d**. In contrast, H···F contacts to the second H atom do not conform to a pattern; they are weaker and may be intramolecular, as in **1b** and **1d**, or intermolecular, such as in **1c**.[30] In the solid-state structure of compound **1d**, an intramolecular aryl−perfluoroaryl interaction is also apparent. Within each molecule of **1d**, the phenyl ring overlaps one of the C_6F_5 rings (interplanar distance ca. 3.26 Å); on the opposite side, there is a symmetry-related Ph ring at a distance of 3.62 Å.[31]

Similar bifurcated intramolecular hydrogen-bonding arrangements, in which each H has two short H···F contacts, are found in each of the secondary amine adducts, **1e**−**g**. The molecular structures of the new examples **1g** and **1h** are presented in Figures 6 and 7, and the hydrogen-bonding data for all four are presented in Table 4. The agreement between the H···F distances in all four compounds (six independent molecules) is striking; in the bifurcated interaction, the average H···F distance is 2.12, 2.11, 2.13, and 2.12 Å for **1e**, **1f**, **1g**, and **1h**, respectively. The largest individual variations are found in **1h** (2.22 and 2.02 Å), where the asymmetry is presumably a consequence of accommodating the sterically bulky benzyl groups.

In contrast to the borane complexes of the primary amine adducts of $Al(C_6F_5)_3$ we have structurally characterized, only **2b** (Figure 8) exhibits a short H(4b)···F(36) contact (2.14 Å). The structure differs significantly from that of **1b**, in that there is no bifurcation and it is the second hydrogen that exhibits a medium-length contact, H(4a)···F(12) (2.28 Å) to another *o*-F. Any intramolecular hydrogen bonding in molecules of **2c** and **2d** (Figure 9) is very weak, and while in each molecule one of the H atoms has a medium-length contact to an *o*-F, the next closest contact is intermolecular

(28) $H_3P{\cdot}B(C_6F_5)_3$ crystallizes with two independent molecules, neither of which exhibits close intramolecular H···F contacts, but there is an intermolecular interaction at 2.39 Å: Bradley, D. C.; Hursthouse, M. B.; Motevalli, M.; Zheng, D. H. *J. Chem. Soc., Chem. Commun*. **1991**, 7.

(29) Remarkably similar bifurcated intramolecular hydrogen-bonding arrangements were observed in 2,6-bis(2,6-difluorophenyl)piperidines: Pham, M.; Gdaniec, M.; Poloñski, T. *J. Org. Chem*. **1998**, *63*, 3731.

(30) ^{t}Bu(H)$_2$P·B(C$_6$F$_5$)$_3$ crystallizes with two independent molecules, each of which has one medium-length intramolecular H···F contact (2.337 and 2.357 Å): Bradley, D. C.; Harding, I. S.; Keefe, A. D.; Motevalli, M.; Zheng, D. H. *J. Chem. Soc., Dalton Trans.* **1996**, 3931.

(31) Favorable intra- and intermolecular interactions between the complementary quadrupoles of fluoroaryl and hydroaryl groups are well-known. See: Reference 7e and references therein.

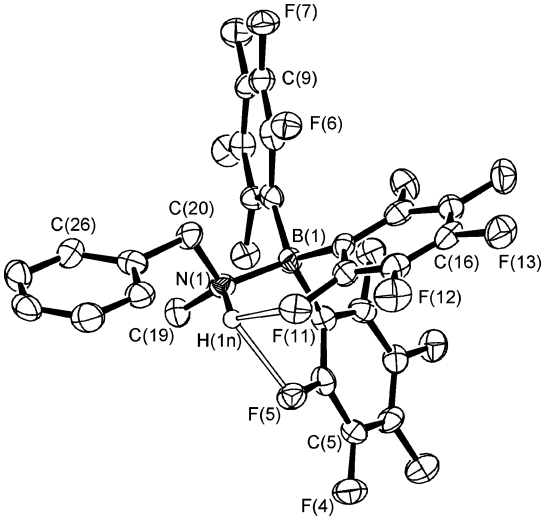

Figure 6. Molecular structure of **1g** with displacement ellipsoids at the 50% probability level. C-bonded H atoms are omitted for clarity.

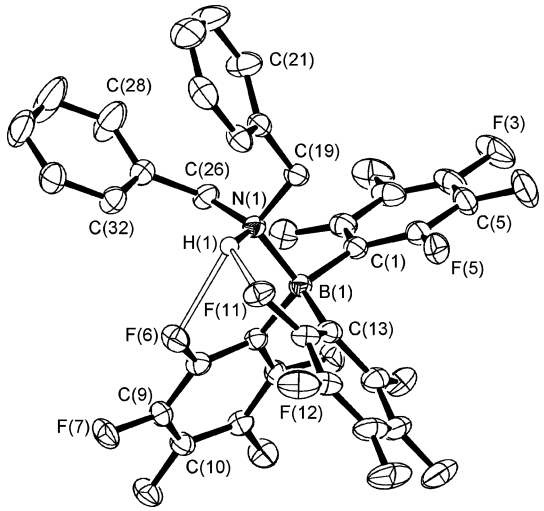

Figure 7. Molecular structure of **1h** with displacement ellipsoids at the 50% probability level. C-bonded H atoms are omitted for clarity.

(see the Supporting Information). Similarly to **1d**, in **2d** the ring of the phenyl group C(3−8) is flanked on both sides by the overlapping and approximately parallel rings of the C_6F_5 groups C(21−26) and C(21′-26′), arranged in infinite stacks parallel to the *a* axis in an ABAB... fashion.[31]

The solid-state structure of each of the secondary amine alane adducts **2e** and **2f** consists of at least two crystallographically independent molecules. In **2e**, there are four independent molecules [**2e**(1)−**2e**(4)]. Those of Al(1) (Figure 10) and Al(4) have very similar conformations, while those of Al(2) and Al(3) also have very similar conformations. The principal differences between the two pairs are in the torsion angles about the Al−N bond; for example, the angles corresponding to C(1)−Al(1)−N(1)−C(20) in the four molecules are 177.62(2), −168.0(3), −177.5(2), and 174.6(2)°. Correspondingly, the intramolecular hydrogen-bonding arrangements are different: in each of molecules 2 and 3, there is a medium H···F contact, 2.20 and 2.26 Å, whereas the shortest in 1 and 4 are 2.36 and 2.38 Å. In all molecules, there are also rather longer H···F contacts, both intramolecular (from 2.47 Å in molecule 3) and intermolecular (2.34−2.58 Å in the four molecules). These intermolecular interactions form one-dimensional columns (Figure 11).

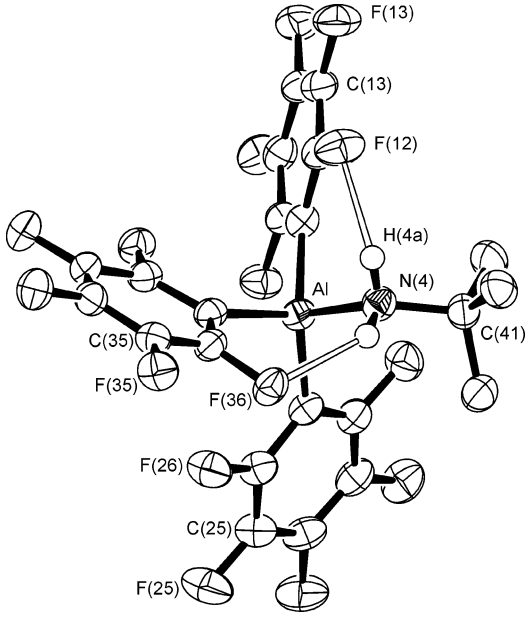

Figure 8. Molecular structure of **2b** with displacement ellipsoids at the 50% probability level. C-bonded H atoms are omitted for clarity.

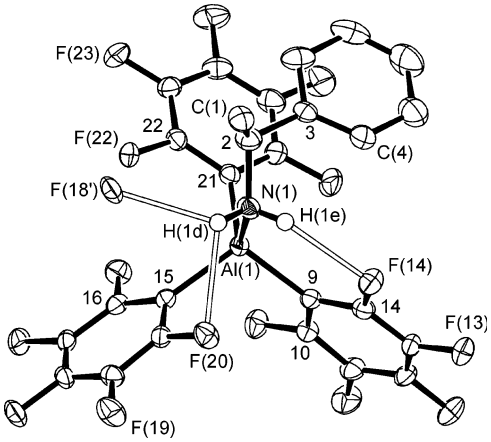

Figure 9. Molecular structure of **2d** with displacement ellipsoids at the 50% probability level. C-bonded H atoms are omitted for clarity.

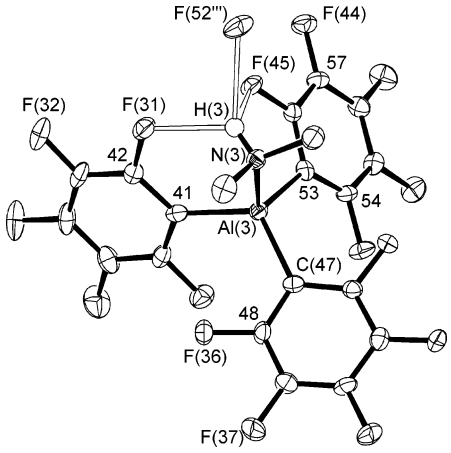

Figure 10. Structure of one of the four independent molecules of **2e** with displacement ellipsoids at the 50% probability level. C-bonded H atoms are omitted for clarity.

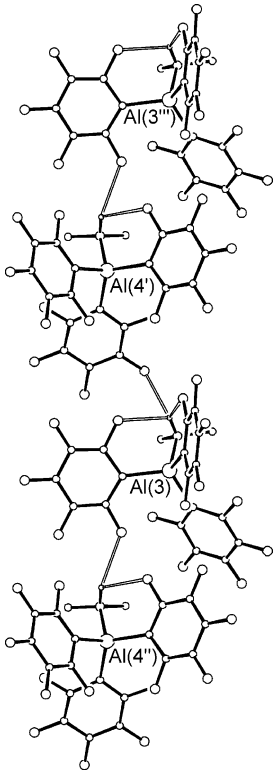

Figure 11. One-dimensional column formed by intermolecular H···F interactions between one of the pairs of molecules in **2e**.

The solid-state structure of **2f** (Figure 12) contains two very similar molecules, each with two intramolecular H···F interactions, and no significant intermolecular H···F interactions. In this instance, the hydrogen-bonding arrangement resembles that of **1f** with a bifurcated F···H···F interaction. However, while in **1f**, the average H···F distance was 2.10 Å, in **2f**, the average distance, over both molecules, is 2.35 Å.

The two molecules of **2g** are quite different. While molecule 1 (Figure 13) has a single medium-length contact, molecule 2 has a very weak bifurcated interaction.

Solution Structures: Variable-Temperature ^{19}F NMR Spectroscopy

Variable-temperature ^{19}F NMR spectroscopy has been demonstrated to be useful in determining the presence and nature of N−H···F−C interactions in solution. Earlier, we employed variable-temperature ^{19}F NMR to deduce a bifurcated hydrogen-bonding pattern in **1b**, and this has now been established as the solid-state structure.[14] The room temperature ^{19}F NMR (toluene-d_8) spectra of **1c** and **1d** (Figure 14a) exhibit a single *o*-F resonance at δ −134.8 and −134.0, respectively. The characteristic splitting and indicative high-field shift of a hydrogen-bond-accepting *o*-F is apparent only at lower temperatures.[14] For **1c**, cooling to −60 °C gives rise to broad *o*-F resonances [δ −132.4 (4F) and −139 (2F)], while at −60 °C, **1d** shows six unique *o*-F's (δ −129.3, −130.5, −131.7, −134.8, −135.6, and −142.6; Figure 14b), a pattern that is consistent with the asymmetric bifurcated arrangement seen in the solid.

For the secondary amine adducts **1e**−**h**, hindered rotation is apparent at room temperature. The ^{19}F NMR spectrum of

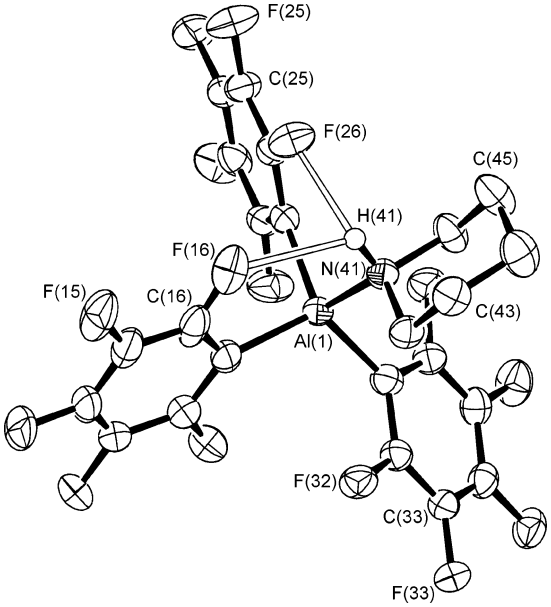

Figure 12. Structure of one of the two molecules of **2f** with displacement ellipsoids at the 50% probability level. C-bonded H atoms are omitted for clarity.

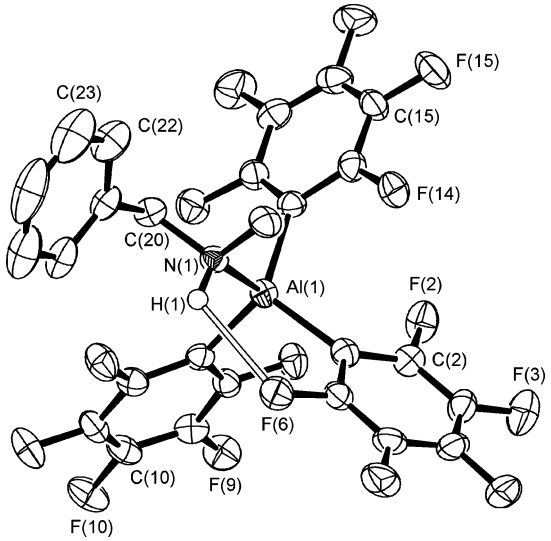

Figure 13. Structure of one of the two independent molecules of **2g** with displacement ellipsoids at the 50% probability level. C-bonded H atoms are omitted for clarity.

1h has three *o*-F resonances in a 2:2:2 ratio (Figure 15), a pattern similar to what we reported for **1e**.[14] We therefore propose that the bifurcated hydrogen bonds present in the solid state are maintained in solution. The hydrogen-bonding interaction makes a significant contribution to the barrier to free rotation, and the effect is not merely steric. This is apparent from the observation that the ^{19}F NMR spectrum of the Et_2MeN adduct does not exhibit decoalescence down to −80 °C.[14] In addition, the coalescence temperature for the significantly more bulky $(PhCH_2)_2NH$ adduct (80 °C), **1h**, is similar to that of the Me_2NH adduct (75 °C), **1e**. The pattern of chemical shifts observed for **1g** is similar to that for **1h**, but in this case, the inherent asymmetry renders all of the *o*-F resonances inequivalent and those interacting with N−H are found at δ −140.0 and −142.8. In contrast to **1b**−

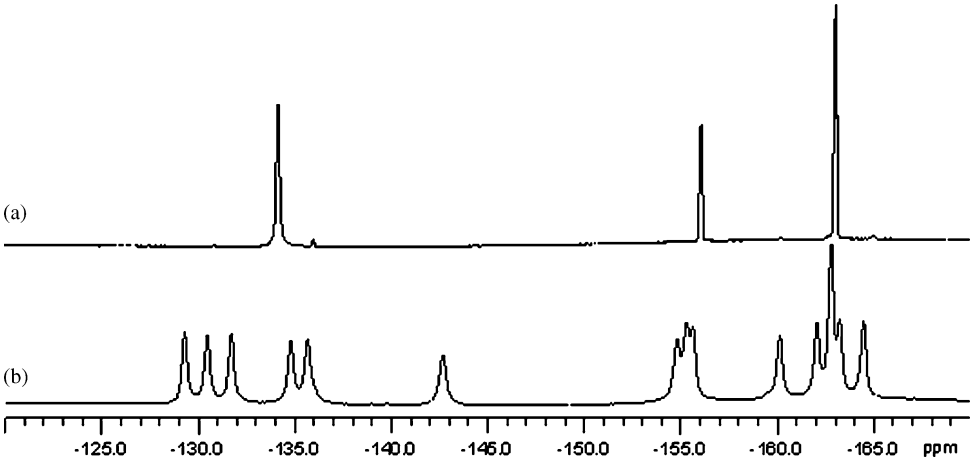

Figure 14. ^{19}F NMR spectra for compound **1d**: (a) toluene-d_8, 20 °C; (b) toluene-d_8, −60 °C.

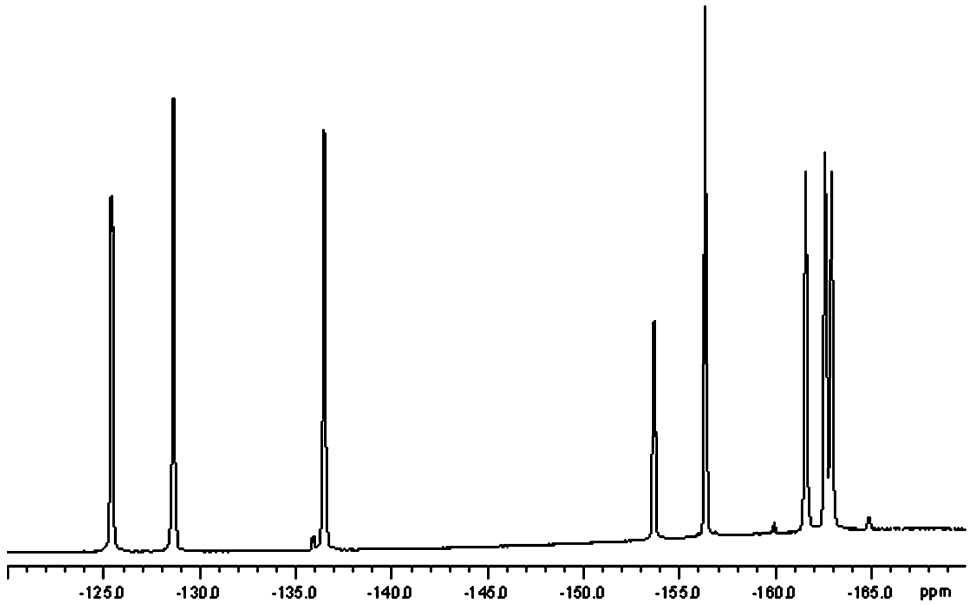

Figure 15. ^{19}F NMR (benzene-d_6, 20 °C) for complex **1h**.

h, the room temperature ^{19}F NMR spectra of both the secondary and primary amine adducts of $Al(C_6F_5)_3$ show only one well-resolved *o*-F resonance, suggesting weaker hydrogen bonding and less hindrance to rotation about the M−N bond. Only at temperatures below −65 °C does the *o*-F resonance of **2e** begin to broaden and subsequently decoalesce, whereas **2b** shows no sign of decoalescence down to −80 °C.

In agreement with the supposition that a bifurcated interaction is required to significantly inhibit rotation, even on cooling to −80 °C, the *o*-F resonances of **1a** broaden but do not decoalesce.

Discussion

Despite the well-documented poor hydrogen-bond-accepting ability of fluorine, since our recognition of short intramolecular N−H···F−C contacts in the anion **III**, we have encountered many further examples. If it is indeed the case, as recent investigations of X−H···F−C interactions have concluded, that they have the characteristics of weak hydrogen bonds,[3d,32] it would seem reasonable that their occurrence might be rationalized using the same approach as hydrogen bonds to more conventional acceptors.

Etter formulated a number of general rules that can be applied to predict the occurrence of hydrogen-bonding interactions: (i) all good proton donors and acceptors are used in hydrogen bonding; (ii) if intramolecular hydrogen bonds completing a six-membered ring are possible, they will usually form in preference to intermolecular hydrogen bonds; (iii) the best proton donors and acceptors remaining after hydrogen-bond formation form intermolecular hydrogen bonds to one another.[33]

The distinctive feature of our compounds is the presence of very good proton donors but poor proton acceptors. In the simplest case, that of the secondary amine adducts, there is only one NH function to serve as a proton donor. Application of rule ii allows us to predict the formation of a six-membered ring and intramolecular hydrogen bonding

(32) For an estimation of the strength of a O−H···F−C hydrogen bond, see: Takemura, H.; Kotoku, M.; Yasutake, M.; Sinmyozu, T. *Eur. J. Org. Chem.* **2004**, 2019.
(33) Etter, M. *J. Phys. Chem.* **1991**, *95*, 4601.

Chart 2

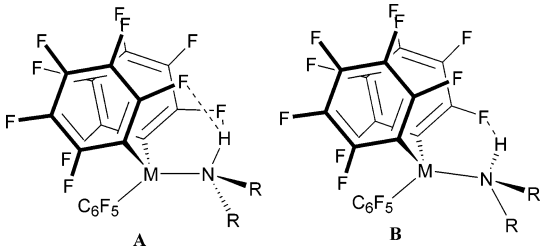

to an *o*-F. Amino hydrogens are known to participate in three-center (bifurcated) hydrogen bonds,[33] so we would therefore predict the formation of either structure **A** or **B** (Chart 2).

For the borane adducts **1e**−**h**, the B−N bond is short enough to allow a favorable bifurcated intramolecular hydrogen-bonding interaction between the NH proton and the two *o*-F's of the form illustrated by **A**. However, accommodating the bifurcated arrangement does cause a noticeable distortion of the tetrahedral geometry at boron, so that in the two independent molecules of **1e** the C−B−C angles between the two C_6F_5 rings participating in hydrogen bonding are 105.7(3)° and 105.4(3)°, whereas the other C−B−C angles between C_6F_5 rings are 113.4(3)° and 115.3(3)° in molecule 1 and 114.1(3)° and 115.2(3)° in molecule 2.

For primary amine adducts, where there are two potential hydrogen-bond donors, one can envisage the possible intramolecular hydrogen-bonding patterns represented by **C**−**E** (Chart 3).

One might have expected that **1b** would adopt structure **C**, in which there are two two-centered intramolecular hydrogen bonds. However, our spectroscopic studies had indicated a bifurcated intramolecular hydrogen-bonding arrangement (structure **D**) in solution. The similarities in the solid-state structures of **1b**−**d** serve to confirm that the bifurcated interaction is indeed more favorable. It follows from Etter's rules that the second proton donor should also participate in intramolecular hydrogen bonding, giving rise to structure **E**. However, the spatial arrangement is much less favorable, and the balance between intramolecular (**1b** and **1d**) and intermolecular (**1c**) interactions is finely poised; because the resulting contact distances to this second hydrogen exceed the Dunitz criteria, we are reluctant to label them hydrogen bonds.

The potential hydrogen-bond donors and acceptors in the aluminum adducts are likely to have properties very similar to those of their boron analogues. However, while we have found three-centered hydrogen bonds with two short−medium N−H···F−C contacts in all of the primary and secondary borane adducts, the H···F contacts are generally rather longer in the aluminum compounds, and there is a greater likelihood of finding intermolecular interactions. The existence of at least two molecules in the solid-state structures of each of the secondary amine adducts of $Al(C_6F_5)_3$, in which there is a significant variation in the intramolecular H···F contacts, suggests that these interactions are weak and easily deformed by competing packing forces.

We believe these differences result principally from the difference in size between the boron and aluminum atoms. In our complexes, the average Al−N bond length (1.97 Å) is 0.33 Å longer than the average B−N bond length (1.64 Å), and similarly for Al−C, it is 1.99 versus 1.64 Å in B−C, a difference of 0.35 Å.

The prevailing picture in the secondary amine adducts of $Al(C_6F_5)_3$ is of a medium-length intramolecular H···F contact and a second longer H···F contact, which may be intra- or intermolecular. There is no discernible pattern in the primary amine adducts of $Al(C_6F_5)_3$. Compound **2b** is interesting because it forms two two-centered hydrogen bonds and adopts structure **C**. In contrast, each molecule of **2c** and **2d** has only medium-length H···F contacts.

Conclusion

Rather than being rare, N−H···F−C interactions short enough and with sufficiently obtuse angles to merit classification as hydrogen bonds are common to all of the protic amine adducts of $B(C_6F_5)_3$ that we have structurally characterized. Compounds of this type are favorably disposed to form six-membered rings through intramolecular hydrogen bonds. If one accepts that organofluorine can function as an (albeit poor) hydrogen-bond acceptor, then the arrangements observed are consistent with Etter's rules. These intramolecular hydrogen bonds to organofluorine are particularly strong where two fluorines connect to a single NH functionality, to give a C−F···H···F−C arrangement. In such cases, they can have a formative influence on the molecular geometry and dynamics, in some cases giving observable effects in room temperature solution NMR spectra.

The corresponding aluminum compounds do exhibit N−H···F−C interactions, but there are fewer and weaker intramolecular contacts, along with an increased tendency for intermolecular over intramolecular interactions, which we ascribe to the greater Al−N bond length, disfavoring the formation of intramolecular hydrogen bonds.

Experimental Section

General Procedures. All syntheses and manipulations were carried out using standard Schlenk techniques. Solvents were distilled under a dinitrogen atmosphere over sodium (toluene), Na/K alloy [light petroleum (bp 40−60 °C)], or CaH_2 (dichloromethane). All NMR experiments were conducted in benzene-d_6 at 20 °C unless otherwise stated. Benzene-d_6, toluene-d_8, dichloromethane-d_2, and chloroform-d_1 were degassed and dried over activated 4 Å molecular sieves. NMR spectra were recorded on a Bruker DPX300 spectrometer. Chemical shifts for ^{1}H NMR spectra were referenced to residual solvent resonances and reported as parts per million relative to tetramethylsilane. ^{19}F and ^{11}B NMR spectra are reported relative to $CFCl_3$ and $Et_2O{\cdot}BF_3$, respectively. $B(C_6F_5)_3$ and $Al(C_6F_5)_3{\cdot}C_7H_8$ were prepared according to the literature procedures.[22,34] The amines **1b**−**h** were purchased from Aldrich and dried over activated 4 Å molecular sieves. The syntheses of compounds **1b**, **1e**, and **1f** have been reported elsewhere.[14,15]

Crystal Structure Analyses. Intensity data for the samples examined were measured either at UEA on a Rigaku/MSC R-Axis-

(34) Lancaster, S. J. http://www.syntheticpages.org/pages/215.

Chart 3

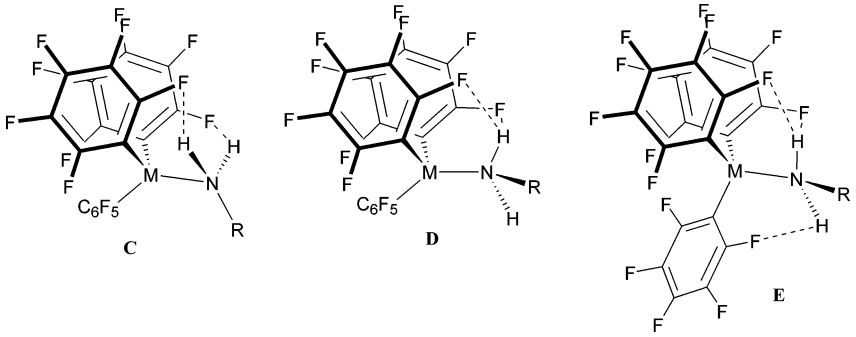

Table 5. Selected Crystal and Structure Refinement Data for the Boron Compounds[a]

compd no.	**1a**	**1a**·NH_3	**1b**	**1c**	**1d**	**1g**	**1h**
formula	$C_{18}H_3BF_{15}N$	$C_{18}H_3BF_{15}N{\cdot}H_3N$	$C_{22}H_{11}BF_{15}N$	$C_{25}H_9BF_{15}N$	$C_{26}H_{11}BF_{15}N{\cdot}CH_2Cl_2$	$C_{26}H_{11}BF_{15}N$	$C_{32}H_{15}BF_{15}N$
fw	529.0	546.1	585.1	619.1	718.1	633.2	709.3
color, habit	colorless, slab	colorless, prism	colorless, shard	colorless, plate	colorless, prism	colorless, blade	colorless, block
cryst syst	triclinic	monoclinic	triclinic	monoclinic	monoclinic	monoclinic	monoclinic
space group	$P\bar{1}$ (No. 2)	$P2_1/n$ (No. 14)	$P\bar{1}$ (No. 2)	$C2/c$ (No. 15)	$P2_1/n$ (No. 14)	$P2_1/n$ (No. 14)	$C2/c$ (No. 15)
a, Å	8.3329(5)	12.1321(10)	10.92740(10)	22.507(5)	10.736(2)	9.5496(12)	22.8044(4)
b, Å	12.9478(8)	12.6612(13)	12.0071(2)	8.9216(18)	8.7560(18)	20.022(3)	13.2282(3)
c, Å	16.3878(7)	13.5485(10)	17.2015(3)	22.773(5)	29.330(6)	12.4075(12)	23.0749(5)
α, deg	86.481(5)	90	83.0820(10)	90	90	90	90
β, deg	85.386(4)	114.066(6)	79.1170(10)	98.91(3)	96.60(3)	94.894(7)	116.9070(10)
γ, deg	89.509(5)	90	77.6070(10)	90	90	90	90
V (Å^3)	1759.06(17)	1900.2(3)	2157.18(6)	4517.6(16)	2738.9(10)	2363.6(5)	6207.2(2)
Z	4	4	4	8	4	4	8
d, calcd (g cm^{-3})	1.998	1.909	1.802	1.821	1.741	1.779	1.518
abs coeff (mm^{-1})	0.229	0.217	0.196	0.193	0.361	0.187	0.152
no. of unique reflns, R_{int}	8031, 0.030	4360, 0.044	9839, 0.077	5160, 0.043	4288, 0.079	5118, 0.251	7081, 0.049
no. of obsd reflns ($I > 2\sigma_I$)	6536	2162	7609	4468	3213	2270	5106
R1 (obsd reflns)	0.035	0.050	0.045	0.037	0.075	0.100	0.046
wR2 (all reflns)	0.092	0.150	0.114	0.097	0.236	0.194	0.134

[a] Data were obtained at 120 K for all but **1d** (140 K).

Table 6. Selected Crystal and Structure Refinement Data for the Aluminum Compounds[a]

compd no.	**2b**	**2c**	**2d**	**2e**	**2f**	**2g**
formula	$C_{22}H_{11}AlF_{15}N$	$C_{25}H_9AlF_{15}N$	$C_{26}H_{11}AlF_{15}N$	$C_{20}H_7AlF_{15}N$	$C_{23}H_{11}AlF_{15}N$	$C_{26}H_{11}AlF_{15}N$
fw	601.3	635.3	649.3	573.3	613.3	649.3
color, habit	colorless, prism	colorless, block	colorless, slab	colorless, block	colorless, prism	colorless, shard
cryst syst	monoclinic	triclinic	triclinic	monoclinic	monoclinic	monoclinic
space group	$C2/c$ (No. 15)	$P\bar{1}$ (No. 2)	$P\bar{1}$ (No. 2)	$P2_1$ (No. 4)	$P2_1/c$ (No. 14)	$P2_1/c$ (No. 14)
a, Å	18.451(4)	13.724(3)	7.9878(3)	15.6465(5)	21.346(4)	21.3404(8)
b, Å	12.842(3)	13.825(3)	11.9032(5)	13.1990(4)	10.968(2)	12.7062(5)
c, Å	19.911(4)	15.012(3)	12.8855(4)	20.3427(7)	22.090(4)	20.2308(7)
α, deg	90	65.61(3)	87.946(2)	90	90	90
β, deg	102.43(3)	85.10(3)	85.528(2)	94.5110(10)	108.95(3)	111.726(2)
γ, deg	90	83.27(3)	87.136(2)	90	90	90
V (Å^3)	4607.3(16)	2574.2(9)	1219.27(8)	4188.1(2)	4891.6(17)	5096.0(3)
Z	8	4	2	8	8	8
d, calcd (g cm^{-3})	1.734	1.639	1.769	1.818	1.666	1.693
abs coeff (mm^{-1})	0.222	0.204	0.218	0.240	0.211	0.208
no. of unique reflns, R_{int}	4213, 0.069	11757, 0.031	5544, 0.055	13572, 0.048	8691, 0.057	11624, 0.097
no. of obsd reflns ($I > 2\sigma_I$)	3514	9259	3831	11341	7053	5655
R1 (obsd reflns)	0.042	0.045	0.052	0.044	0.037	0.052
wR2 (all reflns)	0.117	0.136	0.128	0.109	0.101	0.118

[a] Data were obtained at 120 K for all but **2b** and **2f** (140 K).

IIc image-plate diffractometer equipped with a rotating-anode X-ray source or by the EPSRC Crystallography Service at the University of Southampton on a Nonius Kappa CCD diffractometer. Both systems used monochromated Mo Kα radiation. Crystal data for the boron compounds are collated in Table 5 and those for the aluminum compounds in Table 6. The procedures of the analyses were very similar, and that for compound **1d** is described here.

From a sample of clear, colorless prisms of **1d** under oil, one, ca. 0.8 × 0.15 × 0.10 mm, was mounted on a glass fiber and fixed in the cold nitrogen stream on the Rigaku R-Axis-IIc image-plate diffractometer. The total number of reflections recorded, to $\theta_{max} = 25.4°$, was 12 120, of which 4288 were unique ($R_{int} = 0.079$); 3213 were "observed" with $I > 2\sigma(I)$.

Data were processed using the DENZO/SCALEPACK programs.[35] The structure was determined by the direct method routines in the SHELXS program and refined by full-matrix least-squares

(35) Otwinowski, Z.; Minor, W. *Methods Enzymol.* **1997**, *276*, 307.

methods, on F^2's, in SHELXL.[36] The non-hydrogen atoms were refined with anisotropic thermal parameters. Hydrogen atoms were included in idealized positions, and their U_{iso} values were set to ride on the U_{eq} values of the parent carbon atoms.

In the final difference map, the highest peaks (to ca. 0.67 e Å^{-3}) were close to the solvent (CH_2Cl_2) molecule.

Scattering factors for neutral atoms were taken from ref 37. Computer programs used in this analysis have been noted above, in Table 4 of ref 38, or in ref 39 and were run on a Silicon Graphics Indy at the University of East Anglia or a DEC-AlphaStation 200 4/100 in the Biological Chemistry Department, John Innes Centre.

$H_3N{\cdot}B(C_6F_5)_3{\cdot}NH_3$ (1a·H_3N). NH_3(g) was bubbled through a solution of $B(C_6F_5)_3$ (0.63 g, 1.2 mmol) in light petroleum (40 mL) for 5 min at room temperature. The resulting precipitate was separated by filtration and subsequently recrystallized from a dichloromethane/light petroleum mixture to give colorless needle-shaped crystals, which were confirmed as **1a**·NH_3 by elemental analysis and X-ray crystallography (0.63 g, 1.2 mmol, 94%). Anal. Calcd (found) for $C_{18}H_6BF_{15}N_2$: C, 39.59 (39.63); H, 1.11 (1.16); N, 5.13 (4.32). ^{1}H NMR: δ 3.71 (br, 3H, NH_3), −0.57 (s, 3H, NH_3). ^{11}B NMR: δ −7.1. ^{19}F NMR: δ −135.3 (d, 6F, J_{FF} = 22.6 Hz, *o*-F), −155.8 (t, 3F, J_{FF} = 19.8 Hz, *p*-F), −163.1 (m, 6F, *m*-F). IR: ν(N−H) 3395.5, 3372.5, 3361.8, 3330.2, and 3295.6 cm^{-1}.

$H_3N{\cdot}B(C_6F_5)_3$ (1a). **1a**·NH_3 (0.67 g, 1.2 mmol) was dissolved in ca. 5 mL of toluene before the product was taken to dryness under vacuum. The colorless solid was recrystallized from a light petroleum/dichloromethane mixture cooled to −25°C, giving block-shaped crystals from which the solid-state structure could be determined (0.61 g, 1.2 mmol, 94%). Anal. Calcd (found) for $C_{18}H_3BF_{15}N$: C, 40.87 (40.83); H, 0.57 (0.52); N, 2.65 (3.05). ^{1}H NMR: δ 2.67 (br, 3H, NH_3). ^{11}B NMR: δ −6.9. ^{19}F NMR: δ −135.3 (d, 6F, J_{FF} = 22.6 Hz, *o*-F), −155.5 (t, 3F, J_{FF} = 19.8 Hz, *p*-F), −162.9 (m, 6F, *m*-F). IR: ν(N−H) 3372.5, 3362.0, and 3295.8 cm^{-1}.

$H_2(CH_2C_6H_5)N{\cdot}B(C_6F_5)_3$ (1c). To a solution of $B(C_6F_5)_3$ (1.0 g, 2.0 mmol) in toluene (10 mL) was added H_2NCH_2Ph (0.21 g, 2.0 mmol). The solvent was then removed under reduced pressure, affording a colorless solid that gave single crystals suitable for X-ray crystallography by the slow diffusion of light petroleum through a dichloromethane solution of the product (0.99 g, 1.6 mmol, 80%). Anal. Calcd (found) for $C_{25}H_9BF_{15}N$: C, 48.50 (48.11); H, 1.47 (1.47); N, 2.26 (2.05). ^{1}H NMR: δ 7.00−6.60 (m, 5H, C_6H_5), 4.42 (br, 2H, NH_2), 3.05 (m, 2H, CH_2). ^{13}C NMR: δ 133.8, 129.9 (C_6H_5), 48.9 (CH_2). ^{11}B NMR: δ −4.2. ^{19}F NMR: δ −134.8 (d, 6F, J_{FF} = 22.6 Hz, *o*-F), −155.3 (t, 3F, J_{FF} = 20.8 Hz, *p*-F), −162.4 (m, 6F, *m*-F). IR: ν(N−H) 3337.3 and 3281.8 cm^{-1}.

$H_2{}^tBuN{\cdot}Al(C_6F_5)_3$ (2b). To a solution of $Al(C_6F_5)_3{\cdot}C_7H_8$ (1.74 g, 2.8 mmol) in toluene (20 mL) was added H_2N^tBu (0.20 g, 2.8 mmol) at room temperature. After a few minutes, the solvent was removed under vacuum and the resultant solid was recrystallized from a light petroleum/dichloromethane mixture to give **2b** as X-ray-quality colorless crystals (1.30 g, 2.2 mmol, 77%). Anal. Calcd (found) for $C_{22}H_{11}AlF_{15}N$: C, 43.95 (43.73); H, 1.84 (1.81); N, 2.33 (2.28). ^{1}H NMR: δ 3.92 (s, 2H, NH_2), 1.38 (s, 9H, C(CH_3)$_3$). ^{13}C NMR: δ 149.8, 141.5, 136.9 (C_6F_5), 55.4 (*C*(CH$_3$)$_3$), 30.1 (C(*C*H$_3$)$_3$). ^{19}F NMR: δ −160.7 (m, 6F, *o*-F), −122.4 (m, 3F, *p*-F), −151.9 (m, 6F, *m*-F). IR: ν(N−H) 3299.1 and 3253.6 cm^{-1}.

Acknowledgment. We are grateful to the Engineering and Physical Sciences Research Council for a studentship (A.J.M.) and access to the National Crystallography Service at the University of Southampton.

Supporting Information Available: CIF data and figures illustrating the solid-state structures of **1e**, **1f**, and **2c** as well as synthetic procedures and spectroscopic data for compounds **1d**, **1f**−**h**, and **2c**−**g**. This material is available free of charge via the Internet at http://pubs.acs.org.

IC050663N

(36) Sheldrick, G. M. *SHELX-97—Program for crystal structure determination (SHELXS) and refinement (SHELXL)*; University of Göttingen, Göttingen, Germany, 1997. At the conclusion of the refinement, wR2 = 0.236 and R1 = 0.092 for all 4288 reflections weighted $w = [\sigma^2(F_o^2) + (0.123P)^2 + 6.82P]^{-1}$ with $P = (F_o^2 + 2F_c^2)/3$; for the "observed" data only, R1 = 0.075.

(37) *International Tables for X-ray Crystallography*; Kluwer Academic Publishers: Dordrecht, The Netherlands, 1992; Vol. C, pp 193, 219, and 500.

(38) Anderson, S. N.; Richards, R. L.; Hughes, D. L. *J. Chem. Soc., Dalton Trans.* **1986**, 245.

(39) Sheldrick, G. M. *SHELXTL package, including XS (for structure determination), XL (structure refinement) and XP (molecular graphics)*; Siemens Analytical Inc.: Madison, WI, 1995.